

Supporting Information

Observation of Yu-Shiba-Rusinov State Originated from Magnetic Moment in Curved Monolayer Island of 1T-Phase NbSe₂

Hossain Mohammad Ikram^{1,3*}, *Ara Ferdous*^{1,2}, *Shahed Syed Mohammad Fakruddin*^{1,2}, *Zhipeng Wang*^{1,3}, and *Tadahiro Komeda*^{2*}

¹⁾Department of Chemistry, Graduate School of Science, Tohoku University, 6-3, Aramaki Aza-Aoba, Aoba-ku, Sendai 980-8578, Japan

²⁾Institute of Multidisciplinary Research for Advanced Materials (IMRAM, Tagen), Tohoku University, 2-1-1, Katahira, Aoba-Ku, Sendai 980-0877, Japan

³⁾ Center for Spintronics Research Network, Tohoku University, 2-1-1 Katahira, Aoba-ku, Sendai 980-8577, JAPAN

*Corresponding Author: tadahiro.komeda.a1@tohoku.ac.jp

Table of contents

1. Conversion from 2H to 1T bytunneling current injection
2. Fitting of the STS near the Fermi level
3. Results of the fitting along with lines A, B, and D of Figure 4 of the main text
4. STS plots along with line C of Figure 4 of the main text and the results of the fitting
5. Example of curvature enhanced YSR states
6. Estimation of the strain accumulated in the curved surface

1. Conversion from 2H to 1T bytunneling current injection

We examined the STM-induced conversion from the 2H phase to the 1T phase by applying the pulse voltage of 3 V.

We first found a large flat surface of the 2H phase with the 3×3 reconstruction, originated from the CDW phase. We then applied the pulse voltage of 3V for 100 ms. The STM image after the pulse application is shown in Figure S1(a). In the upper-part of the image, we can observe the superstructure of $\sqrt{13} \times \sqrt{13}$ R13.9°, which is characteristic to the surface reconstruction of the CDW 1T phase.^{1, 2} The height difference of these two phases is illustrated in Figure S1(b) as the cross-sectional height plot. The left-hand side corresponds to the 1T domain where a corrugation of 0.4 Å originated from the reconstruction appears. The 2H phase domain shows no such corrugation. There is no height shift between the planes of the 2H and 1T phases.

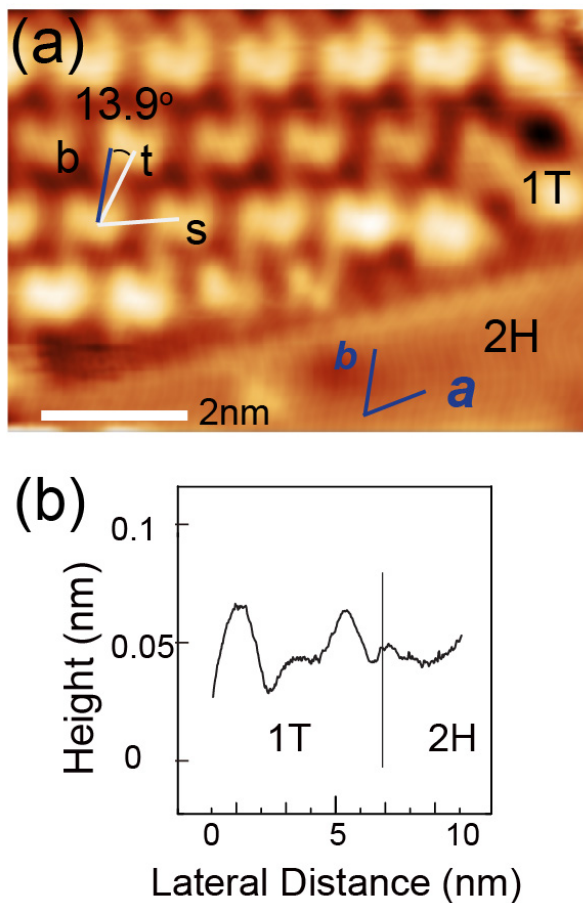


Figure S1. (a) The STM image of the NbSe₂ surface. The lower-right corner is the original 2H phase, and upper-left region is the converted 1T reconstructed surface. (b) Height profile along the phase boundary of 1T-2H.

2. Fitting of the STS near the Fermi level

The STS spectra are numerically fitted by dividing into components of SC-gap and Lorentzian peaks with the following equation of (1).

$$F(x) = \frac{1}{\exp(\frac{D-|V|}{K})+H} + \sum_i \frac{A_i}{1+(\frac{V-P_i}{W_i})^2} \quad \text{---eq. s1)}$$

The first term of eq. (1) was supposed to simulate the staircase of the trough of the SC gap, where $\pm D$ is the position of the gap-edges, K is the steepness of the gap, and H is the trough height. The Lorentzian function appeared in the second term of eq. 1) is for the QP peak and YSR peaks.

The actual fitting was done by using the following formula.

$$y=y0+1/(\exp((D-sqrt(x^2))/K)+H)+A1/(1+((x-P1)/W1)^2)+A2/(1+((x+P1)/W2)^2)+A3/(1+((x-P2)/W3)^2)+A4/(1+((x+P2)/W4)^2)+A5/(1+((x-P3)/W5)^2)+A6/(1+((x+P3)/W6)^2)$$

3. Results of the fitting along with lines A, B, and D of Figure 4 of the main text

The parameters obtained by the fitting are listed below along lines A,B, and D.

Table S1

Fitting parameters along line A

	A1	A2	A3	A4	A5	A6	A7	A8	A9	A10	A11	A12	A13
y0	-0.39	-0.39	-0.38	-0.39	-0.37	-0.4	-0.44	-0.88	-0.55	-0.49	-0.6	-0.38	-0.4
D	1.13	1.13	1.13	1.13	1.13	1.13	1.13	1.13	1.13	1.13	1.13	1.12	1.13
K	0.034	0.041	0.112	0.125	0.141	0.13	0.117	0.162	0.139	0.048	0.096	0.144	0.01
H	2.761	2.586	2.789	2.848	3.025	2.854	2.604	1.34	2.082	2.538	1.997	2.998	2.814
A1	0.898	0.829	0.681	0.54	0.376	0.186	0.249	0.148	0.01	0.01	0.01	0.468	0.158
A2	0.908	0.893	0.624	0.368	0.244	0.053	0.113	0.016	0.051	0.01	0.01	0.335	0.125
A3	0.05	0.1	0.05	0.748	0.924	1.593	1.048	0.259	0.105	1.504	0.747	0.726	0.761
A4	0.05	0.098	0.05	0.837	0.845	1.239	0.818	0.112	0.01	0.602	0.127	0.563	0.738
A5	0.033	0.005	0.014	0.075	0.127	0.416	0.869	8	3.349	2.991	3.865	0.01	0.01
A6	0.005	0.02	0.005	0.01	0.151	0.576	1.054	5.868	2.387	2.065	2.666	0.284	0.114
P1	1	1.005	1.005	1.05	1.051	1.049	1.056	1.05	1.044	1.04	1.05	1.131	1.13
P2	0.886	0.903	0.887	0.848	0.838	0.844	0.869	0.88	0.871	0.826	0.858	0.857	0.986
P3	0.65	0.6	0.58	0.53	0.5	0.455	0.456	0.467	0.491	0.556	0.581	0.617	0.65
W1	0.13	0.136	0.153	0.139	0.136	0.073	0.1	0.061	0.05	0.05	1	0.167	0.142
W2	0.119	0.123	0.132	0.128	0.098	0.122	0.073	0.236	0.051	0.05	0.05	0.149	0.064
W3	0.059	0.058	0.05	0.093	0.091	0.082	0.083	0.067	0.05	0.05	0.05	0.085	0.183
W4	0.05	0.05	0.071	0.1	0.087	0.077	0.074	0.379	0.05	0.053	0.155	0.111	0.149
W5	1	0.836	1	0.019	0.05	0.059	0.064	0.059	0.072	0.063	0.064	0.05	0.08
W6	0.05	1	0.05	0.012	0.05	0.072	0.073	0.07	0.101	0.102	0.088	0.063	0.089

Table S2

Fitting parameters along line B

	B1	B2	B3	B4	B5	B7	B8	B9	B10	B11	B12
y0	-0.43	-0.37	-0.38	-0.38	-0.39	-0.42	-0.41	-0.4	-0.39	-0.36	-0.39
D	1.13	1.13	1.13	1.13	1.13	1.13	1.13	1.13	1.13	1.13	1.13
K	0.023	0.024	0.073	0.023	0.019	0.01	0.03	0.022	0.025	0.074	0.062
H	2.518	2.675	2.638	2.826	2.862	2.668	2.778	2.594	2.711	2.923	2.651
A1	0.832	0.929	0.37	0.675	0.798	0.693	0.377	0.596	0.935	0.539	0.481
A2	1.002	0.84	0.06	0.563	0.398	0.526	0.298	0.533	0.79	0.058	0.333
A3	0.483	0.212	0.604	0.386	0.412	0.592	0.592	0.34	0.244	0.391	0.369
A4	0.233	0.344	0.791	0.549	0.678	0.474	0.548	0.374	0.408	0.783	0.452
A5	0.078	1.00E-04	0.01	0.424	0.2	0.525	0.42	0.251	0.01	0.005	0
A6	0	0.013	0.043	0.395	0.311	0.747	1.127	0.537	0.16	0.005	0
P1	1.049	1.029	1.127	1.041	1.052	1.05	1.05	1.05	1.05	1.13	1.13
P2	0.936	0.915	0.977	0.908	0.906	0.922	0.97	0.945	0.938	0.984	0.974
P3	0.6	0.6	0.599	0.615	0.57	0.578	0.677	0.685	0.637	0.7	0.7
W1	0.104	0.124	0.155	0.116	0.123	0.073	0.091	0.094	0.133	0.166	0.195
W2	0.139	0.113	0.116	0.09	0.067	0.065	0.069	0.094	0.102	0.05	0.151
W3	0.082	0.055	0.104	0.073	0.081	0.083	0.1	0.066	0.067	0.075	0.086
W4	0.058	0.066	0.151	0.105	0.127	0.1	0.088	0.083	0.083	0.127	0.108
W5	0.948	0.01	0.01	0.086	0.071	0.116	0.135	0.263	0.05	0.005	0
W6	0.001	0.046	0.017	0.081	0.089	0.129	0.086	0.099	0.098	0.005	0

Table S3

Fitting parameters along line D

	D1	D2	D3	D4	D5	D6	D7	D8	D9	D10	D11	D12	D13
y0	-0.42	-0.44	-0.43	-0.4	-0.43	-0.38	-0.42	-0.51	-0.42	-0.4	-0.36	-0.38	-0.39
D	1.13	1.13	1.13	1.13	1.13	1.13	1.13	1.13	1.13	1.13	1.13	1.13	1.13
K	0.105	0.032	0.186	0.01	0.072	0.032	0.141	0.473	0.383	0.232	0.152	0.1	0.051
H	2.552	2.312	2.435	2.998	2.653	2.93	2.74	2.061	2.516	2.938	3.244	3.214	2.966
A1	0.571	0.775	0.588	0.995	0.465	0.763	0.644	0.053	0.152	0.076	0.122	0.07	0
A2	0.58	0.74	0.533	0.632	0.509	0.92	0.212	0.01	0.051	0.01	0.028	0.01	0.008
A3	0.1	0.05	0.297	0.737	0.258	0.01	1.022	1.691	1.705	1.988	1.089	1.197	0.032
A4	0.1	0.005	0.107	0.614	0.024	0.178	0.842	1.012	1.136	1.469	1.008	1.169	0
A5	0.005	0.05	0.125	0.188	1.499	0.596	0.467	0.107	0.01	0.01	0.01	0.113	0.525
A6	0.005	0.027	0.118	0.127	1.504	0.585	0.861	0.768	0.198	0.247	0.01	0.01	2.94
P1	1.109	1.01	1.016	1.016	1.013	1.006	0.945	1	1.13	1.13	1.13	1.13	1.13
P2	0.955	0.891	0.845	0.85	0.85	0.85	0.87	0.882	0.841	0.855	0.889	0.928	1
P3	0.58	0.55	0.598	0.579	0.556	0.564	0.514	0.576	0.58	0.59	0.61	0.63	0.639
W1	0.278	0.157	0.204	0.124	0.156	0.116	0.106	0.144	0.2	1	0.103	0.05	0.999
W2	0.24	0.132	0.134	0.079	0.123	0.122	0.099	0.05	0.062	0.05	0.05	0.05	1
W3	0.069	0.075	0.055	0.073	0.05	1	0.066	0.087	0.079	0.08	0.123	0.105	0.05
W4	0.068	0.05	0.069	0.101	0.05	0.05	0.081	0.075	0.086	0.062	0.121	0.143	0.093
W5	0.05	1	0.05	0.05	0.074	0.089	0.065	0.05	0.01	0.05	0.05	0.317	0.16
W6	0.05	0.813	0.062	0.06	0.078	0.074	0.115	0.097	0.043	0.105	0.05	0.05	0.086

4. Position dependent STS along with line C and the results of fitting

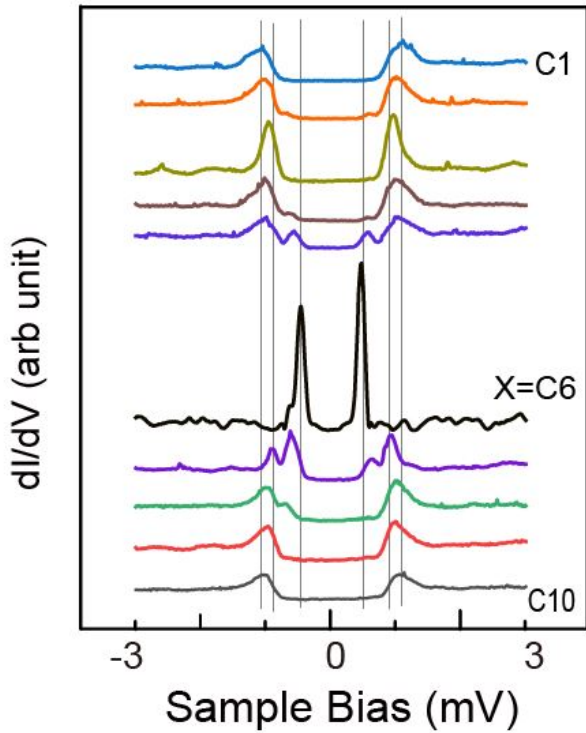


Figure S2. STS variation along with line C of Figure 4 of the main text.

Table S4

Fitting parameters along with line C

	C1	C2	C3	C4	C5	C6	C7	C8	C9	C10
y0	-0.44	-0.41	-0.36	-0.41	-0.37	-0.88	-0.38	-0.36	-0.39	-0.36
D	1.13	1.13	1.13	1.13	1.13	1.13	1.13	1.13	1.13	1.13
K	0.083	0.028	0.111	0.039	0.027	0.162	0.05	0.026	0.041	0.073
H	2.475	2.625	3.37	2.703	3.008	1.34	3.164	2.947	2.818	2.891
A1	0.403	0.757	0.377	0.293	0.665	0.148	7.00E-48	0.641	0.175	0.398
A2	0.368	0.867	0.337	0.357	0.649	0.016	0.055	0.491	0.182	0.356
A3	0.416	0.408	1.253	0.764	0.105	0.259	1.036	0.474	0.795	0.389
A4	0.378	0.286	1.219	0.712	0.223	0.112	0.661	0.505	0.768	0.487
A5	0.078	0.037	0	0.005	0.324	8	0.419	0.495	0.049	0.021
A6	0.001	0.04	0	0.116	0.368	5.868	1.071	0.31	0	0
P1	1.13	1.03	1.05	1.079	1.019	1.05	1.04	1.045	1.091	1.106
P2	0.974	0.915	0.938	0.961	0.875	0.88	0.918	0.932	0.963	0.972
P3	0.7	0.69	0.75	0.614	0.564	0.467	0.607	0.692	0.7	0.7
W1	0.158	0.128	0.098	0.135	0.148	0.061	0.885	0.107	0.094	0.154
W2	0.127	0.134	0.05	0.105	0.102	0.236	0.012	0.08	0.057	0.125
W3	0.119	0.083	0.098	0.14	0.052	0.067	0.108	0.094	0.117	0.094
W4	0.099	0.034	0.09	0.11	0.066	0.379	0.075	0.09	0.109	0.091
W5	1	1	0.001	0.001	0.084	0.059	0.096	0	1	1
W6	0.001	0.029	0.001	0.085	0.087	0.07	0.106	0.101	0.05	0.05

5. Example of curvature enhanced YSR states

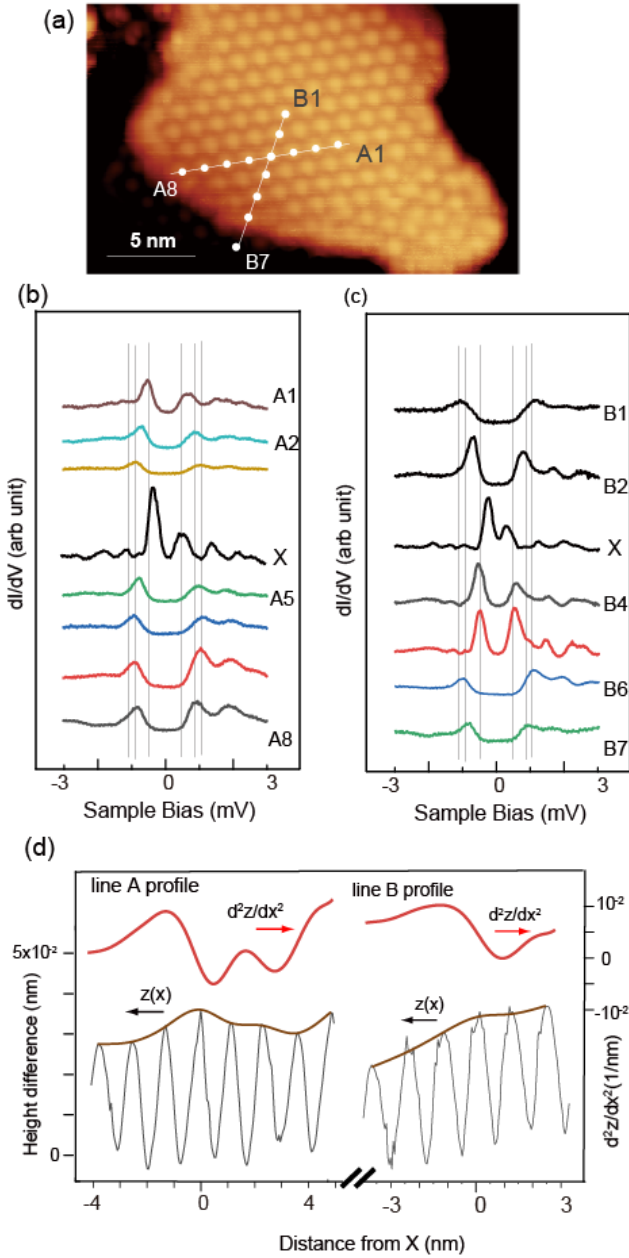


Figure S3 (a) Positions of STS measurement on the surface of Fig. 2(a) island. A1-A8 and B1-B7 are defined along the unit vectors of $\sqrt{13} \times \sqrt{13}$ R13.9°. (b),(c) STS spectra obtained at points along lines A and B, respectively. (d) (lower) Cross-sectional height profile along lines A and B with envelope function $z(x)$ in brown. (upper) $d^2z(x)/dx^2$ plots in red.

We show another example of the position dependence of the peculiar YSR peak observed for the 1T island (see Figure S3(a)). The STS spectra were obtained along the

lines A and B, and the measurement points are sequentially named A1-A8 and B1-B7. The island is identical to that shown in Figure 2(a) of the main manuscript. The STS showed the YSR peaks around a particular point marked \times . We show the results obtained along the lines A and B in Figures S3(b) and (c), respectively. The superimposed vertical lines are identical to those in Figure 5(a) of the main text, representing the positions of the QP, Y1, and Y2. At \times , the YSR peak dominates the spectrum and appears at the energy of Y1. Note that the STS are sensitive to a minute difference in the measurement position, and there is a slight difference in the spectra at the identical \times in Figures S3(b) and (c). The local curvature is shown in (d) for the directions of A and B.

Along both lines, we see a slight bump at position \times . Accordingly, we see the minimum d^2z/dx^2 at position \times . The energy position of the YSR peaks has a good correlation with the film curvature, and the former approach the Fermi level with the latter's increase. The correlation of the amount of J estimated from the YSR position with the local curvature supports our assumption that the magnetic moment appears with the help of the film curvature, which is superimposed on the magnetization expected from the reconstructed 1T phase.

6. Estimation of the strain accumulated in the curved surface.

Here we consider a model to estimate the strain. As the possible origin of the appearance of the strain on the 1T film, it should be noted that the calculated lattice constant of 1T and 2H phases are different from each other. The profile of the 1T layer is specified as $f(x)$ in Figure S4(a). The transition layer has a Se-Se spacing of L_h in the lower side and $L_h + \Delta L_h$ on the upper side, contacting with 1T layer with the Se-Se layer spacing of L_v . (see Figure S4(b)) The equation can be converted into the following relation.

$$\Delta L_h/L_h = f'' L_v$$

The left-hand term corresponds to the transition layer's strain from the 2H state. Using the f'' value of -7×10^{-3} estimated in the main text, $L_v = 0.33$ nm, and $L_h = 0.34$ nm, we obtain the tensile strain of 0.26 %. It was estimated 0.5-1.0 % of lattice mismatch between 2H and 1T,³, which indicates the above estimation is realistic.

Zhou and coworkers showed that a few tenths of μ_B are accumulated by the biaxial tensile strain of 1% for the magnetic moment strength created by the strain.⁴ The estimated strain produces a magnetic moment that is smaller than 0.1 μ_B . However, the YSR signal can probe this much of the magnetic field.

The tensile strain is an order of magnitude smaller than those previously reported in the strain-induced magnetic moment studies. However, the created magnetic moment is detected by YSR states, which implies a possibility of precise control of the local magnetic field and applications to the device operation. Combined with the ability of the STM to fabricate the 1T phase locally and manipulate the folding of the 1T layer, the technique shown in this article should be further explored for the method to manipulate and analyze the local magnetic moment.

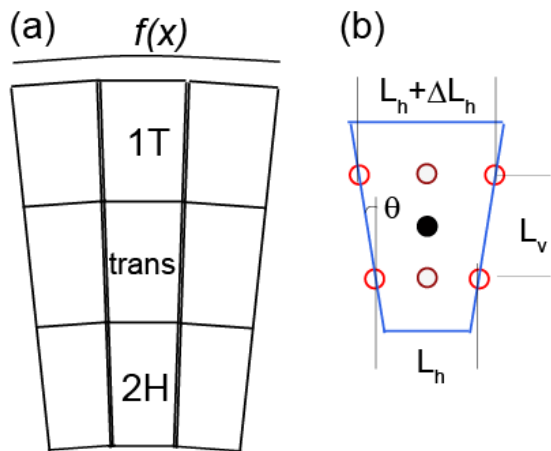


Figure S4 Elastic models of the strain accumulated in the interface between 1T and 2H layers. (a) Illustration of the 1T, 2H, and transition region. The top-line describes the curvature expressed as $f(x)$. (b) The dimensions of the lattice relaxation.

References

- s1. F. Bischoff, W. Auwärter, J. V. Barth, A. Schiffrin, M. Fuhrer and B. Weber, *Chem. Mater.*, 2017, **29**, 9907-9914.
- s2. H. Wang, J. Lee, M. Dreyer and B. I. Barker, *J. Phys. Condens. Matter*, 2009, **21**, 265005.
- s3. C. Tresca and M. Calandra, *2D Materials*, 2019, **6**, 035041.
- s4. Y. Zhou, Z. Wang, P. Yang, X. Zu, L. Yang, X. Sun and F. Gao, *ACS Nano*, 2012, **6**, 9727-9736.